Int J Adv Manuf Technol (2015) 78:1445–1453
DOI 10.1007/s00170-014-6740-4

ORIGINAL ARTICLE

# PCD tool performance in high-speed milling of high volume fraction SiCp/Al composites

**Tao Wang · Lijing Xie · Xibin Wang · Zhiwei Ding**

Received: 26 July 2014 / Accepted: 18 December 2014 / Published online: 10 January 2015


**Abstract** This paper presents a systematical study on polycrystalline diamond (PCD) tool performance during high-speed milling of high volume fraction (65 %) and small size (nominal size 10 μm) SiC particle-reinforced aluminum, which is rarely reported before. The influence of milling parameters (milling speed and feed rate) and PCD particle size on tool wear were investigated. The results indicated that the tool wear increased dramatically with the milling speed, and it was not suitable to mill the material above 300 m/min for the industrial application. Larger feed rate could achieve larger removed volume before VC reached 0.6 mm, while the pattern reverses in terms of milling time. The optimized PCD particle size is 10 μm. The main wear modes of PCD tool were flank wear and crater wear, and the wear mechanism was analyzed by scanned electronical microscope (SEM), laser scanning microscope (LSM), and Raman spectroscopy.

**Keywords** Aluminum-matrix composites · Milling · Tool wear · Surface roughness · Chip

## 1 Introduction

Silicon carbide particle-reinforced aluminum-matrix composites have been proven superior to conventional materials in terms of high strength to weight ratios, low sensitivity to temperature variations, high stiffness, and wear resistance [1]. These superior properties make this class of material attractive to a wide spectrum of application in the aerospace, automotive, electronics, and medical industries [2]. However, due to the presence of hard SiC particles in the aluminum matrix, machining SiCp/Al composites is encountered with extremely rapid tool wear, thereby increasing tool cost and aggravating the surface integrity. These materials are classified as the difficult-to-machine materials. Although many engineering components made from SiCp/Al composites are produced by the near net shape forming and casting processes, final machining and finishing processes are generally still required to fabricate a MMC component to the final dimensions [3]. Therefore, a widespread industrial application of SiCp/Al composites will not be achieved without appropriate solution to the machining problem.

The machinability of SiCp/Al composites has drawn great academic and scientific attention over the last several decades. Ciftci et al. [4] carried out machining tests on two levels of SiC particles with different mean particle sizes and results indicated that reinforcement particle size and its weight fraction together with the cutting speed were found to be the major factors affecting the tool wear. Weinert and König [5] found that although cutting speed increased from $v_c$=100 m/min using cemented carbide to $v_c$=500 m/min using polycrystalline diamond (PCD) tool, the wear decreased. And tool wear was less when using coarser grained PCD for turning an aluminum alloy with 18 % volume fraction. Davim [6, 7] conducted an experiment on machining composite A356/20/SiCp-T6, included both turning and drilling operation, and obtained the correlation between the cutting force and tool wear. The results indicated that the force information could be an indirect method of monitoring the tool wear. Hung et al. [8] validated several tool wear models and concluded that roughing with uncoated WC inserts and then finishing with PCD tools was the most economical way in machining SiC-reinforced MMCs. Quan and Zhou [9] conducted experiment on cutting 15 wt% SiCp/Al composites and concluded that the cutting composites reinforced by coarse SiC particles required

T. Wang · L. Xie (✉) · X. Wang · Z. Ding
Beijing Institute of Technology, Beijing, China
e-mail: rita_xie2004@163.com

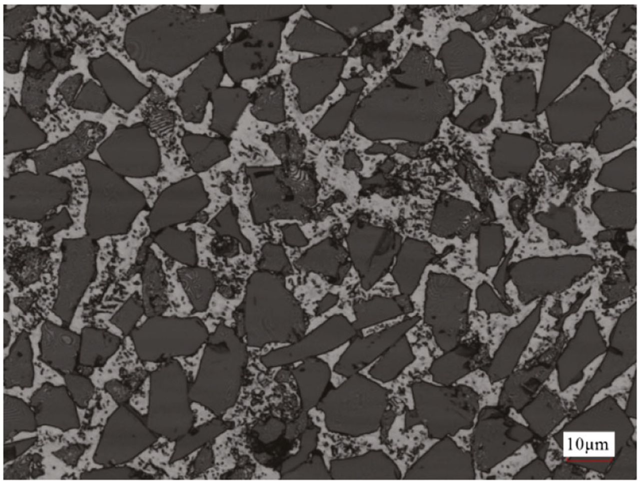


**Fig. 1** Microstructure of the $SiC_p$/Al composites

tools with high hardness, and conventional tools were only adaptable to cut composites reinforced by fine SiC particles. Pedersen and Ramulu [10] used TiCN/TiN-coated carbide cutting tools to study the finish machining of a silicon carbide particle-reinforced magnesium metal matrix composite and observed that a greater depth of cut reduced the amount of tool wear for a given volume of material removed. Li and Seah [11] investigated the effect of reinforcement phases on the machinability characteristics of SiCp/Al composites and concluded that increase volume fraction and average size of the reinforcement phase in MMCs would increase tool wear. The results agree with the conclusions drawn by Ozben et al. [12].

Generally, the majority of the published research focuses on turning of SiCp/Al composites with low volume fraction of reinforcement, i.e., less than 30 %. However, there is a large application of these materials with high reinforcement content in electric packaging such as in satellites due to its low heat expansion and high heat conductivity [13]. In addition, a large portion of the materials in the components are supposed to be removed by milling due to the higher processing efficiency,

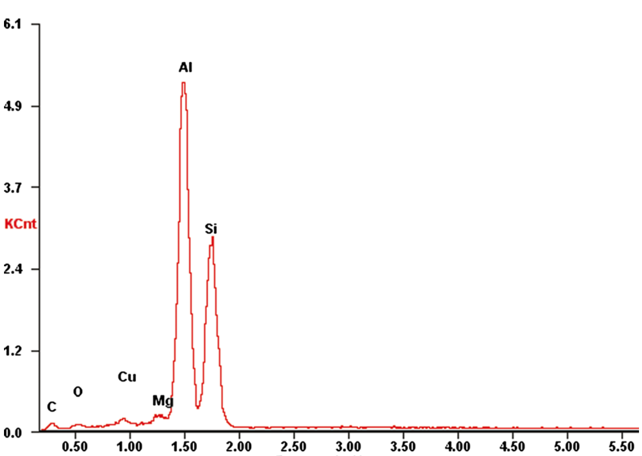


**Fig. 2** Chemical element identification of the machined surface

**Table 1** Properties of SiC/Al composites

| Properties | Value |
|---|---|
| Thermal conductivity (W/mK) | 160–200 |
| Coefficient of thermal expansion ($10^{-6}$/K) | 7–9 |
| Density (g/cm$^3$) | 3.1 |
| Elastic modulus (GPa) | 130 |
| Passion ratio | 0.3 |
| Tensile strength (MPa) | 500 |
| Average size of SiC particles (μm) | 10 |
| Volume fraction of SiC (%) | 65 |

smaller cutting force, lower surface temperature, and better surface quality. Recently, Huang et al. [14] and Bian et al. [15] carried out tests on high-speed milling of high volume fraction 56 and 65 %, respectively. The SiC particle size in their research was relatively large (60 μm).

To the best of the authors' knowledge, the papers about high-speed milling of high volume fraction SiCp/Al composite with small SiC particle size are rarely reported before. Therefore, the primary objective of this paper is to present an experimental study on PCD tool performance during high-speed milling of the material. First, experimental procedure and materials are introduced in Section 2. Then, in Section 3, experimental results and analysis are presented which includes wear curves, surface quality, tool life curve, wear pattern, and mechanism. Finally, the discussion about measurement, temperature, and particle size is proposed for the future research.

## 2 Experimental design and procedure

### 2.1 Materials

High-speed milling tests are conducted on SiCp/Al composite, which is composed of Al6063 aluminum matrix and SiC particle reinforcements and fabricated by vacuum infiltration

**Table 2** Milling conditions

| Items | Contents |
|---|---|
| Insert holder | R217.69-1020.RE-09.2AN (SECO) |
| PCD grain size (μm) | 1, 10, 25 |
| Tool diameter (mm) | 20 |
| Operation | Down milling |
| Cutting condition | Dry milling |
| Cutting speed (m/min) | 100, 300, 400,500 |
| Feed rate (mm/z) | 0.025, 0.05, 0.075, 0.15 |
| Axial depth of cut (mm) | 0.2 |
| Radial depth of cut (mm) | 10 |

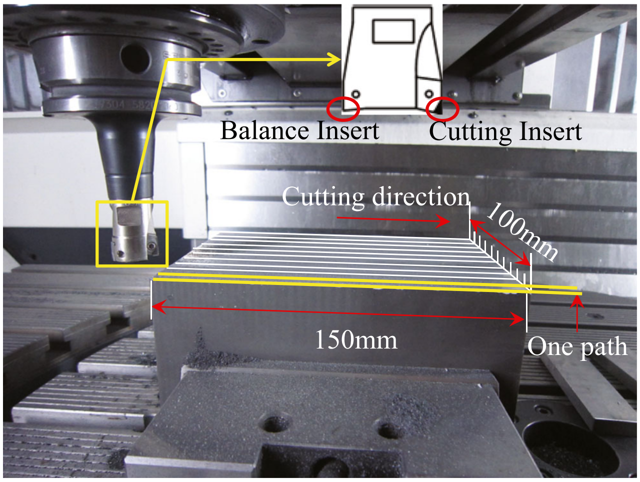


**Fig. 3** he schematic photo of tool wear test during milling process

method. The microstructure and chemical element identification are shown in Figs. 1 and 2, respectively. The dark polyhedral SiC particles with sharp corners instead of round ones are surrounded by bright aluminum matrix. The details material properties are listed in Table 1.

### 2.2 Equipment setup

The machining tests are carried out on a DMU80 monoBLOCK five-axis machining center. Due to the high hardness and severe abrasive characteristics of SiC particles, PCD tools are the most suitable tool material for the machining of SiCp/Al composites [6, 16]. Therefore, the study only focuses on the performance of PCD inserts for the practical requirement. Single-factor experiments are performed for the study on the influence of cutting speed, feed rate, and PCD grain size on tool wear and machined surface roughness, and the milling conditions are listed in Table 2.

### 2.3 Experimental procedure and tool wear measurement

A schematic photo of tool wear test during milling process is demonstrated in Fig. 3. The initial size of workpiece is 150 mm×10 mm×20 mm. Since the removed volume of SiCp/Al composite is more valuable than milling time in practical production, all the horizontal axis in the tool wear curve are recorded as path number and each path, as shown on

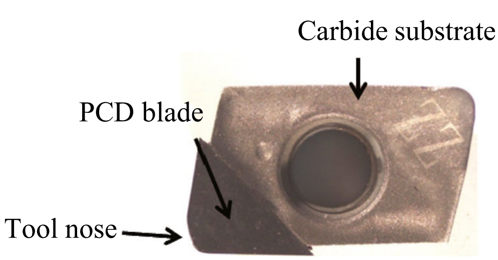


**Fig. 4** A sample of PCD insert

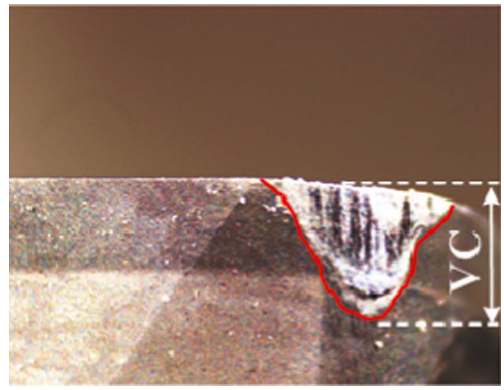


**Fig. 5** The schematic picture of VC measuring method

the top surface of workpiece, has a fixed volume of the removed metal, i.e., 150 mm×10 mm×0.2 mm=300 mm$^3$. In order to avoid the intersection of the side wall, the milling tool moves 10 mm perpendicular to feed direction after each path. In other words, a whole lay of workpiece is removed in 10 paths. All the wear curves in this paper are not as flank wear curve in the ordinary sense which is plotted as a function of cutting time. However, the curve can demonstrate a clearer pattern of the tool performance with respect to the removed volume of the materials from workpiece. Except for the tests on the influence of PCD grain size, the PCD grain size of all the PCD tools is 10 μm.

All tool wear tests are conducted on single-flute PCD insert accompanying by a balance insert, and the latter insert does not participate into cutting process during the tests, as shown in the magnified photo in Fig. 3. The tools are examined by Zeiss Optical Microscope Discovery V12 after each predetermined cutting action until they fail. According to the practical production requirement, the machining accuracy is an important issue. In order to avoid excessive deformation during the milling process, all the axial depth of cutting in the tool wear tests is fixed at 0.2 mm which is similar to the practical milling parameter. The radius of tool noses is 0.8 mm and the tool wear occurrs at the tool nose. The shape of the wear area appears to be an inverted triangle below the corner of the tool, which partially includes the major flank and

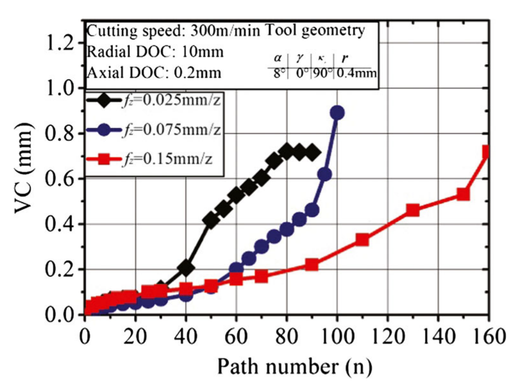


**Fig. 6** The influence of milling speed on tool wear

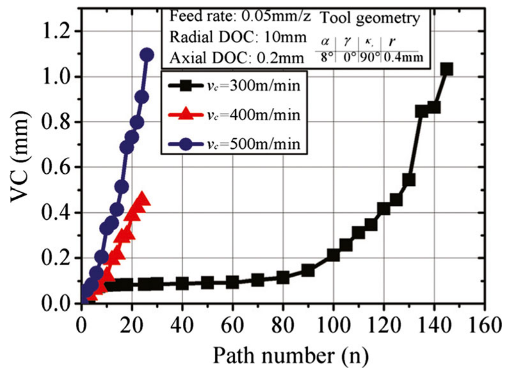


**Fig. 7** The influence of feed rate on tool wear

the minor flank. It indicates that serious radius and flank wear occurred in the PCD tool. Therefore, only maximum wear VC (wear land width of the flank at the tool corner) is recorded which is similar to the record method in [9] and [17]. A sample of the cutting insert and typical schematic of VC measure method are shown in Figs. 4 and 5, respectively.

At the end of each tool wear test, the tool wear characteristics are examined by scanned electronical microscope (SEM), laser scanning microscope (LSM), and Raman spectroscopy. The machined surface roughness measurements are taken in feed direction by a TR240 surface roughness tester, and the final results are obtained by averaging the values from five locations under each milling condition.

## 3 Experimental results

### 3.1 Wear curves

The milling speed has a significant influence on tool performance according to Fig. 6. When milling speed is 400 m/min or higher, the tool wear curve soars with the increasing paths number without a uniform wear period. However, the wear curve experiences a uniform wear period within 90 milling paths when milling speed reduces to 300 m/min. Therefore, it is not suitable to mill SiCp/Al composite at a milling speed of 400 m/min or higher. The main reason is that the increasing speed will exaggerate the abrading action of SiC particles against the cutting tool, thereby reducing tool life. In addition, the heat generated at high speed can be detrimental to both the bonding strength and the hot hardness of the tool, which can lead to the decrease of the wear resistance. The result is in agreement with the early studies by [18] and [19].

The tool wear reduces when feed rate increases from 0.025 to 0.15 mm/z, as demonstrated in Fig. 7. This is consistent with the result reported by [20–22]. According to the analysis by [16], this trend can be attributed to two reasons as follows: (1) when cutting fixed volume material, high feed rate can reduce the contact between the cutting edge and abrasive SiC particles; (2) high feed rate can acquire high thermal temperature in cutting area which makes the workpiece soft, and then the SiC particles tend to be pressed into the workpiece rather than cut through. Therefore, almost all the researchers recommend that feed rate should be as high as possible if it can produce an acceptable surface finish. However, it is worth pointing out that the variation and amplitude of the periodically varying milling force during intermittent cutting process increases with feed rate, which makes the brittle PCD tools more vulnerable to fracture. Therefore, when choosing a higher feed rate value, it should be guaranteed that the severe problem of tool fracture does not occur. In addition, the surface finish deteriorates with an increase in feed. Larger feed results in more damage and also a greater damage depth into the material [23, 24]. Therefore, the surface quality should also be considered when larger feed is chosen in the milling process.

In terms of PCD particle size, the tool with 1-μm-diameter PCD particle does not experience a uniform period and VC value reaches 0.6 mm at around 38 path number, as shown in Fig. 8. As for the tool with 10-μm-diameter PCD particle, the value of path number is around 132 when VC value reaches 0.6 mm, which is almost three times larger than that of 1 μm. This can be attributed to the fact that PCD

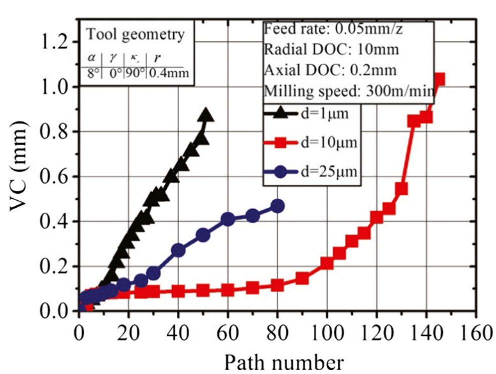


**Fig. 8** The influence of PCD particle size on tool wear

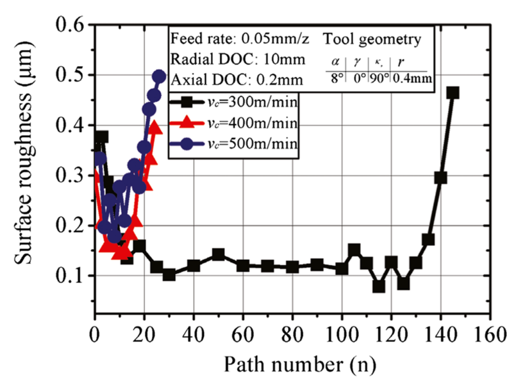


**Fig. 9** The variation of machined surface roughness in different milling speed

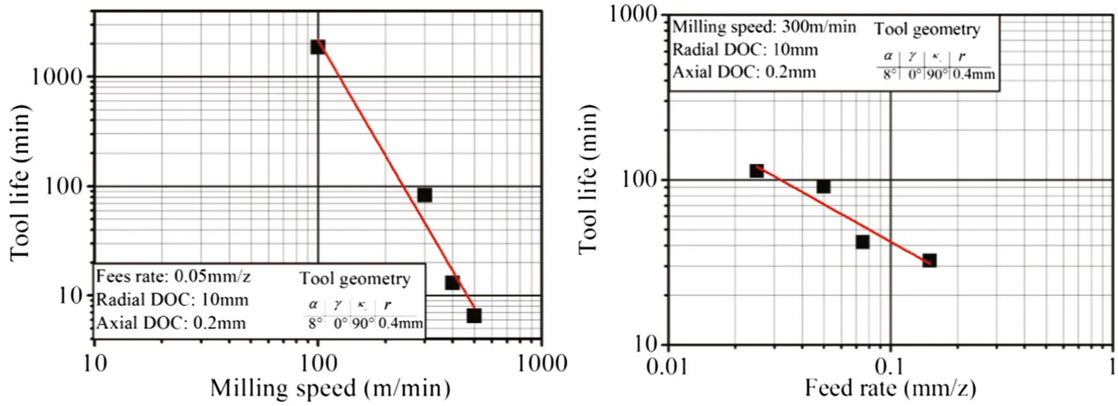


(a) Tool life vs. milling speed (b) Tool life vs. feed rate

**Fig. 10** Taylor Tool life curves for high speed milling of SiCp/Al composite. **a** Tool life vs. milling speed. b Tool life vs. feed rate

with larger diamond particle normally exhibits better abrasion resistance. As the particle size increases further to 25 μm, the PCD particles are supposed to be pulled out during machining more easily, and the machine tool starts to experience vibration after 80 milling paths. Therefore, the optimal PCD grain size is 10 μm in the tests. Lane [19] also studied the performance of different PCD tools' grain size and pointed out that there was an optimal PCD size for the tool which is 25 μm in his research and further increase in PCD grain size did not benefit the tool life, but rather caused significant deterioration in the surface roughness. The different optimal PCD sizes can be attributed to the different volume fractions and particle sizes of SiC which is out of the research scope in this paper.

## 3.2 Surface quality and tool life curve

In order to define an appropriate tool life criterion, i.e., the allowable tool wear value before tool rejection, the influence of path number on the machined surface roughness is investigated, as shown in Fig. 9. With the increase of the milling path number, all the curves in Fig. 8 witness a dramatic drop of surface roughness prior to reaching a low-surface roughness state. There is vast difference among the durations of low-surface roughness state for different milling speeds, and only at 300 m/min, there is the longest and stable low-surface roughness state. Since each new tool wear test started with the poor machined surface generated by the last worn tool and a layer of whole surface can be removed in 10 paths, all the surface roughness value are quite high in the first 10 paths. In the meantime, it is worth mentioning that generally when the VC value reaches around 0.6 mm, the surface roughness starts to experience a dramatic increase. Therefore, the effective tool life could be determined based on the following criteria: (1) VC reaches 0.6 mm and (2) excessive chipping/fracture of the cutting edge occurs.

In the conventional representation of the tool life curve, the log-log scale is utilized in both horizontal and vertical axial so as to achieve an approximate curve in the form of linear function. In this way, tool life curves at different milling speeds and feed rates are shown in Fig. 10 based on the abovementioned tool life criterion, i.e., VC=0.6 mm. In order to get more accurate results, each figure includes one more point based on two new tool wear tests. Tool life decreases dramatically when milling speed increases which consistent with the pattern of tool wear curve. In terms of feed rate, tool life curve witnesses a moderate decrease with the increasing feed rate. It is interesting to find that if the tool life is considered in terms of milling time, a different pattern experiences for feed rate. This apparent contradiction might cause confusion to the consumers and clearly warrants an explanation. An approach based on rewriting the Taylor equation is a good

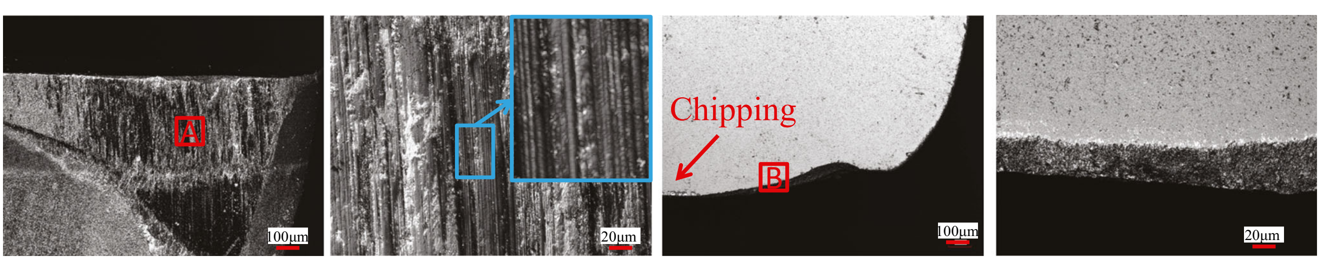


(a) Flank face (b) Magnification A (c) Rake face (d) Magnification B

**Fig. 11** Micrographs of worn tool with 1-μm particle size at VC=0.867 mm. **a** Flank face. **b** Magnification A. **c** Rake face. **d** Magnification B

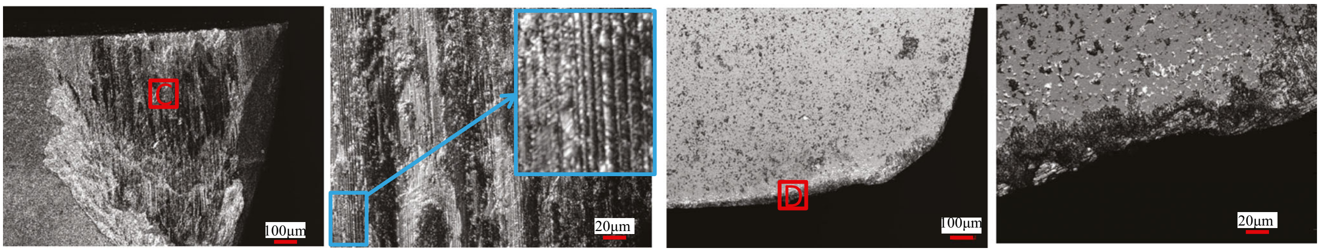


(a) Flank surface (b) Magnification C (c) Rake surface (d) Magnification D

**Fig. 12** Micrographs of worn tool with 10-μm particle size at VC=1.032 mm. **a** Flank surface. b Magnification C. **c** Rake surface. **d** Magnification D

solution and the details can be found in [25]. In order to calculate the tool life at different milling speeds and feed rates, tool life equations are achieved by using least square fitting technique, which are shown:

$$T = 10^{10.32} v_c^{-3.50} R^2 = 0.97 \quad (1)$$

$$T = 10^{0.76} f_z^{-0.87} R^2 = 0.84 \quad (2)$$

3.3 Wear pattern and mechanism

Typical micrographs of the worn tool with 1-, 10-, and 25-μm particle sizes are shown in Figs. 11, 12, and 13, respectively, laser scanning microscope. According to these photos, the prominent failure modes in milling SiCp/Al composite are flank and crater wear. Micro chipping can be witnessed on cutting edge, but it is not severe in the worn tools, as shown in Figs. 11c and 13c. However, the scenario is quite different from the report by [15], in which microchipping and cleavage were witnessed on the tool tip and the tool corner geometry has totally changed due to the wear on tool tip, although the fraction volume of SiC particle is the same. The main reason can be attributed to the different cutting tools and reinforcement size. Specifically, the cutting tool is monocrystalline diamond in [15] and its crystallographic orientation is fixed, while PCD tool in these tests is constituted of numerous tiny diamonds and its crystallographic orientation is random. Therefore, PCD tool has a high hardness (slightly less than monocrystalline diamond), while its toughness and bending strength are higher than monocrystalline diamond according to [26], making microchipping rarely occurred in the test. Furthermore, the SiC particle size in this test is relatively smaller (10 μm) than that of [15] (60–80 μm). Research by [9] indicated that when SiC particle is coarse, it is difficult for the tool to press the SiC particles into the chip or the machined surface due to the large resistance of the matrix. Coarse SiC particles are more likely to turn, break, and fall out which make them scratch on cutting edge more intensively, thereby leading more microchipping in their tests.

In terms of the flank wear, deep grooves parallel to cutting direction can be witnessed on all the three tools, as shown in Figs. 11b, 12b, and 13b, which serve as the typical evidence for abrasive wear. Since the hardness of PCD (8000 HV) is much higher than SiC (3000 HV), the groove phenomenon is unexpected. However, almost all the research on tool wear during cutting SiC-reinforced composite observed abrasive wear on the flank surface. It could be attributed into two main reasons: (1) highly frequent impact and scratch by SiC under high temperature and stress and (2) three-body abrasive wear due to the detached grain PCD from tool and SiC from workpiece. In addition, due to the high temperature and pressure in tertiary cutting zone, the adhered aluminum matrix can be observed on the flank surfaces as well. However, the adhesive wear is not obvious in the flank surface from the images.

In terms of the rake wear, the results from EDS analysis indicate that the rake surface near cutting edge is covered by aluminum matrix. In the meantime, the wear region near the

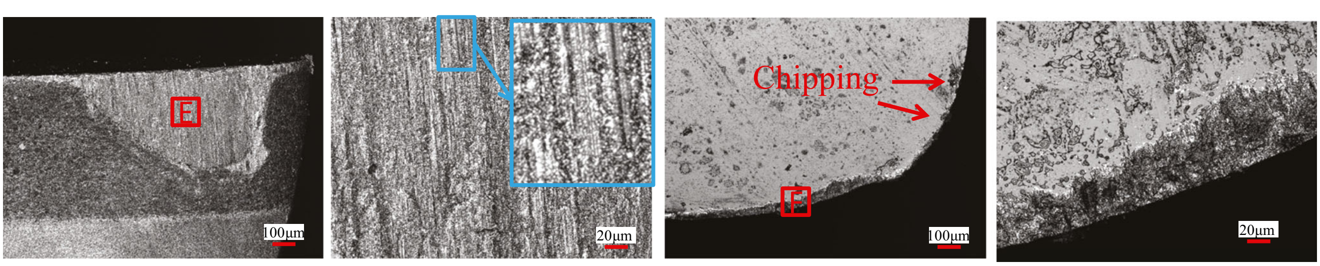


(a) Flank surface (b) Magnification E (c) Rake surface (d) Magnification F

**Fig. 13** Micrographs of worn tool with 25-μm particle size at VC=0.481 mm. **a** Flank surface. **b** Magnification E. **c** Rake surface. **d** Magnification F

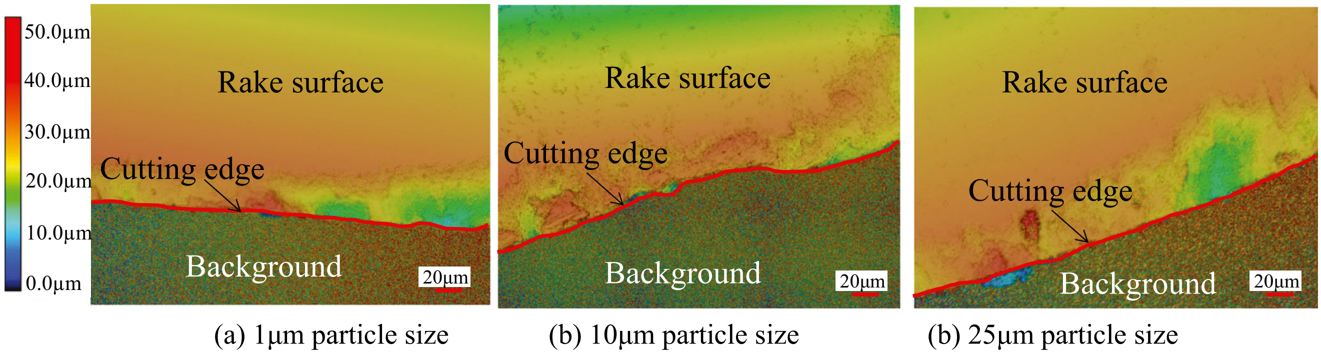


**Fig. 14** The 3D morphology of the worn rake surfaces. **a** 1-µm particle size. **b** 10-µm particle size. **c** 25-µm particle size

cutting edge is quite rough, as shown in Figs. 11d, 12d, and 13d. Therefore, the one wear mechanism can be attributed to adhesive wear. The adhered phenomenon can be more clearly observed in 3D image as shown in Fig. 14. However, the grooves are not obvious in the all three (d) images which are unexpected. In order to provide more information about the rake surface, SEM is utilized to analyze the micromorphology around B, D and F in larger magnification as shown in Fig. 15:

In Fig. 15a, the rake surface is eroded by NaOH solution and the aluminum material is removed. It is interesting to find that there are many pits at the similar size (1 µm) of PCD grain on the wear land, which can be attributed to the pull out of the PCD grain. As for Fig. 14b, c without erosion, although aluminum material can still be observed on the rake surface, there are obvious deep grooves on it, which can serve as the evidence of abrasive wear. The wear process of the rake surface can be described as a cycle consisted of three parts: (1) the new surface is scratched by the hard SiC and detached PCD, thereby generating grooves along cutting direction; (2) due to high temperature and pressure in the milling process, the grooves will be covered by aluminum material soon when milling operation continues; (3) the adhered aluminum material is scratched by SiC and detached PCD, which can lead to the pull out of PCD grain. Then the rough surface will be covered soon again by aluminum material and the cycle goes on and on.

Since PCD tool tends to experience diamond-graphite phase transformation during high-speed milling, Raman spectroscopy was utilized to study the phenomenon on a rake surface of worn PCD tool cutting. As shown in Fig. 16, there is a sharp peak around 1338 $cm^{-1}$ before transformation, which indicates that the diamond content is quite high. However, the peak vanishes on the worn rake surface which means that almost all the diamond on the measured point transformed. In the meantime, it is interesting to find that there are obvious two peaks (1340 and 1580) indicating that the diamond-graphite phase transformation occurred. The results can be attributed to two reasons: (1) The high temperature occurred during high-speed milling, especially when the tool wearing occurred. (2) The metal catalyses exist on rake surface, Co as the binding material of PCD tool and Cu as a component from the workpiece. The research by [27] indicates that copper is the most active for diamond-graphite phase transformation among Ni, Co, Fe, and Ti.

## 4 Discussions

In terms of VC measurement, it is worth pointing out that when VC becomes large as milling test continues, the adhered alumnium film can occur on the flank surface and it exerts great influence on measuring VC value due to the

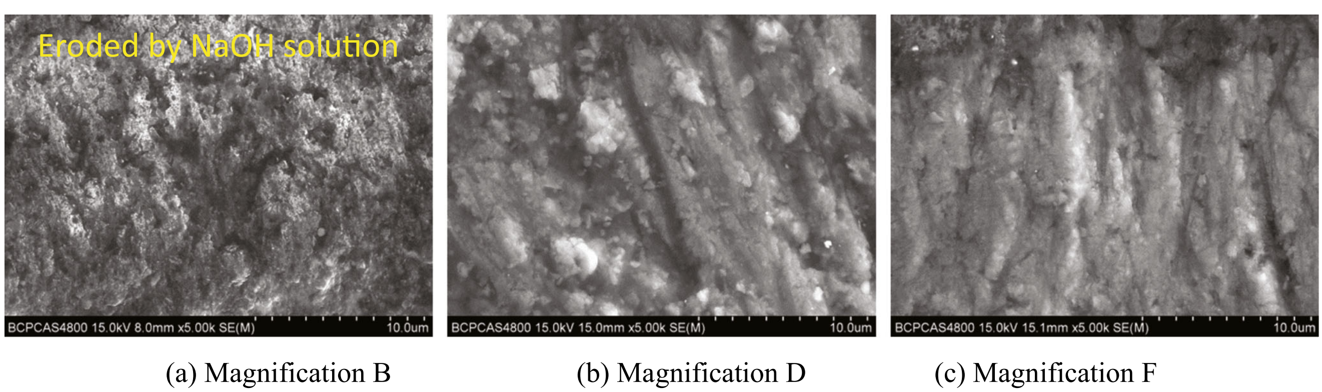


**Fig. 15** Micromorphology of worn rake surface by SEM. **a** Magnification B. **b** Magnification D. **c** Magnification F

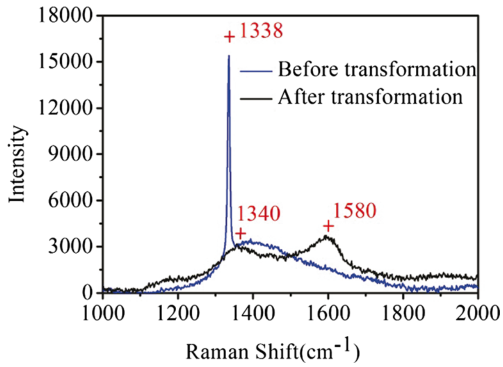


**Fig. 16** Raman spectra measured in rake surface

corresponding difficulty in distinguishing the boundary. Therefore, the accuracy of the wear curve versus path number can be improved if the influence can be eliminated. Research by [17] indicated that the flank wear band-width after etching was in 30 % smaller than that before etching. In addition, two of the tool wear curves stopped recording before VC reached 0.6 mm in the tool wear tests since the vibration of machine tool is out of the normal working range. It is of great value to explore the dynamic feature of the machine tool when high-speed milling the material in the future.

In terms of the temperature during the milling process, it is important to estimate the value since it plays an important role in the diamond-graphite phase trsansformation. As it is known to all, it is quite difficult to measure it accurately through direct experiment methods, some researchers have already explored several new approaches. Ge et al. [26] utlized a theoretical method to estimate the teperature at the interface based on the chip mrophology and the increased temperature could be derived as 505 °C. In their research, the fraction volume of the reinforcement is relatively low (15 %) and the chip was achieved through ultra-precision turning. However, if the fraction volume increases to 65 % and the workpiece is machined by milling rather than turning, the chip is helical and fragile which makes it extremely difficult to achieve the metallographic preparation. The finite element method technique is another promising approach. However, there are a vast number of obstacles. First, it is not appropriate to treat the SiCp/Al composite as an equivalent homogenous material properties, which means that the model should include the material properties of SiC particle and aluminium matrix at the same time. Second, the interface properties between particle and matrix is still an uncertain field which necessitates further investigation. In addition, since the milling processing is mainly accomplished by tool corner (axial depth of cutting is 0.2 mm and the radius value to tool corner is 0.4 mm), the model can not simplizfied into plain-strain model, and only 3D model is suitable, thereby increasing the complexity of the model dramatically.

In terms of the PCD grain size, the individual tools in this test has a fixed size, such as 1 or 25 μm. It is acknowledged that the coarse diamond exhibits greater abrasion resistance and hardness than that of fine diamond, while it usually suffers from relatively low toughness and rough cutting edge. In order to achieve the optimal comprehensive performance of the PCD tool, a promising directions is to combine diamond particle of different sizes (for example, 1 and 25 μm) in the mixture to increase the diamond packing density [28]. It is worth exploring the research on the performance of the mixture size PCD tools milling SiCp/Al composite in the future.

## 5 Conclusions

PCD tool performance during high speed milling of SiCp/Al composite is experimentally investigated in this paper. The volume fraction is 65 % and particle nominal size is 10 μm. The following conclusions can be drawn from above analysis:

For the sake of both machining quality and economy, high-speed milling under a milling speed of 300 m/min with a tool refreshment criterion of VC=0.6 mm is reasonable. By combining with a feed rate less than 0.075 mm/z, a satisfactory machining surface with Ra≤0.4 μm is produced during the whole tool life. It deserves special attention that higher milling speed is followed by shorter tool life and higher frequency of tool replacement.

PCD grain size plays an important role in tool performance. The coarser of the PCD grain, the higher of the abrasion resistance and hardness, whereas the lower of the toughness. Due to the high hardness and frequent impact effect of SiC particles, an optimized PCD grain size is 10 μm, which is on the same level of the nominal size of SiC particles.

The dominated tool wear modes in milling SiCp/Al composite are flank wear and crater wear. In terms of flank face, the main wear mechanism is abrasive wear; while in terms of rake surface, the main wear mechanisms are abrasive and adhesive wear. In addition, the results measured by Raman spectroscopy indicate that diamond-graphite phase transformation occur in the rake surface as well. The phenomenon of microchipping is not severe in PCD tool during all the tests.

**Acknowledgements** This work is supported by the National Key Projects of Science and Technology of China (Item No.: 2012ZX04003051-3).

## References

1. Kannan S, Kishawy HA, Balazinski M (2006) Flank wear progression during machining metal matrix composites. J Manuf Sci E-T Asme 128:787–791
2. Clyne TW, Withers PJ (1993) An introduction to metal matrix composites. Cambridge University Press, Cambridge
3. Davim JP (ed) (2011) Machining of metal matrix composites. Springer, London

4. Ciftci I, Turker M, Seker U (2004) Evaluation of tool wear when machining SiCp-reinforced Al-2014 alloy matrix composites. Materials and Design 25:251–255
5. Weinert K, König W (1993) A consideration of tool wear mechanism when machining metal matrix composites (MMC). Ann CIRP 42(1): 95–98
6. Davim JP, Baptista AM (2000) Relationship between cutting force and PCD cutting tool in machining silicon carbide reinforced aluminium. J Mater Process Technol 103:417–423
7. Davim JP (2001) Turning particulate metal matrix composites. Experimental study of the evolution the cutting forces, tool wear and workpiece surface roughness with the cutting time. Proc Inst Mech Eng B J Eng Manuf 215:371–376
8. Hung NP, Boey FYC, Khor KA, Oh CA, Lee HF (1995) Machinability of cast and powder formed aluminum alloys reinforced with SiC particles. J Maters Process Technol 48: 291–297
9. Quan YM, Zhou ZH (2000) Tool wear and its mechanism for cutting SiC particle-reinforced aluminium matrix composites. J Maters Process Technol 100:194–199
10. Pedersen W, Ramulu R (2006) Facing SiCp/Mg metal matrix composites with carbide tools. J Mater Process Technol 172:417–423
11. Li XP, Seah WKH (2001) Tool wear acceleration in relation to workpiece reinforcement percentage in cutting of metal matrix composites. Wear 247:161–171
12. Ozben TEK, Kilickap E, Cakir O (2008) Investigation of mechanical and machinability properties of SiC particle reinforced Al-MMC. J Mater Process Technol 198:220–225
13. Tan ZH, Pang BJ, Gai BZ, Wu GH, Jia B (2007) The dynamic mechanical response of SiC particulate reinforced 2024 aluminum matrix composites. Mater Lett 61:4606–4609
14. Huang ST, Zhou L, Yu XL, Cui Y (2012) Experimental study of high-speed milling of SiCp/Al composites with PCD tools. Int J Adv Manuf Technol 62:487–493
15. Bian R, He N, Li L, Zhan ZB, Wu Q, Shi ZY (2013) Precision milling of high volume fraction SiCp/Al composites with monocrystalline diamond end mill. Int J Adv Manuf Technol 71:411–419
16. El-Gallab M, Sklad M (1998) Machining of Al:SiC particulate metal-matrix composites Part I: tool performance. J Mater Process Technol 83:151–158
17. Andrewes CJE, Feng HY, Lau MW (2000) Machining of an aluminum/SiC composite using diamond inserts. J Mater Process Technol 102:25–29
18. Chambers AR (1996) The machinability of light alloy MMCs. Compos Part A 27:143–147
19. Lane C (1992) The effect of different reinforcements on PCD tool life for aluminium composites. Proceedings of the machining of Composites Materials Symposium. ASM Material week, Chicago, IL 1–5:17–27
20. Tomac N, Tannessen K, Rasch FO (1992) Machinability of particulate aluminium matrix composites. Ann CIRP 41:55–58
21. Cronjäger L, Meister D (1992) Machining of fibre and particle-reinforced aluminium. Ann CIRP 41:63–66
22. Morin E, Masounave J, Laufer EE (1995) Effect of drill wear on cutting forces in the drilling of metal-matrix composites. Wear 184: 11–16
23. Dabade UA, Dapkekar D, Joshi SS (2009) Modeling of chip-tool interface friction to predict cutting forces in machining of Al/SiCp composites. Int J Mach Tool Manuf 49:690–700
24. El-Gallab M, Sklad M (1998) Machining of Al/SiC particulate metal matrix composites—part II: workpiece surface integrity. J Mater Process Technol 83:277–285
25. Lin JT, Bhattacharyya D, Lane C (1995) Machinability of a silicon carbide reinforced aluminium metal. Wear 181:883–888
26. Ge YF, Xu JH, Yang H (2010) Diamond tools wear and their applicability when ultra-precision turning of SiCp/2009Al matrix composite. Wear 269:699–708
27. Uemura M (2004) An analysis of the catalysis of Fe, Ni or Co on the wear of diamonds. Tribol Int 37:887–892
28. Davim JP (ed) (2008) Machining: fundamentals and recent advances. Springer, London